PHYSICAL REVIEW D **87,** 071501(R) (2013)

Diffraction production in a soft interaction model: Mass distributions

E. Gotsman,[1] E. Levin,[1,2] and U. Maor[1]

[1]*Department of Particle Physics, School of Physics and Astronomy, Raymond and Beverly Sackler Faculty of Exact Science, Tel Aviv University, Tel Aviv 69978, Israel*

[2]*Departamento de Física, Universidad Técnica Federico Santa María, Aenida, España 1680 Valparaíso, Chile and Centro Cientifico-Tecnolgico de Valparaíso, Casilla 110-V, Valparaíso, Chile*

(Received 20 February 2013; published 8 April 2013)

In the framework of the Gotsman-Levin-Maor model for soft interaction with $\alpha'_{\rm IP}(0) = 0$, we propose a procedure based on Gribov's partonic interpretation of the Pomeron, which enables one to calculate the diffractive mass distributions in hadron-hadron scattering. Using the analogy with deep-inelastic scattering, we associate the Pomeron-quark interaction with the Good-Walker sector of the hadron-hadron scattering, and the Pomeron-gluon sector with the t-channel Pomeron interactions. We present predicted mass distributions for the LHC energies.

DOI: 10.1103/PhysRevD.87.071501 PACS numbers: 13.85.−t, 13.85.Hd, 11.55.−m, 11.55.Bq

I. INTRODUCTION

Recently we proposed a model for soft interactions at high energies that provides a good description of the LHC data on total, elastic and diffractive cross sections [1–3], as well as inclusive hadron production [4]. This model incorporates the main features of theoretical approaches to high energy interactions: viz. perturbative QCD [5–8] (pQCD) and N = 4 SYM [9–14]. The resulting features are

(i) A large value of the Pomeron intercept ($\Delta_{\rm IP} \approx 0.2$–$0.3$) and diminishing $\alpha'_{\rm IP} = 0$ (pQCD and N = 4 SYM);
(ii) A large contribution of Good-Walker (GW) [15] mechanism to diffraction production N = 4 SYM);
(iii) Significant triple Pomeron (3IP) interaction (matching with pQCD).

In Table I we show our predictions for the different components of single diffraction production, $\sigma^{\rm GW}_{\rm sd}$ corresponding to the GW mechanism, while $\sigma^{\rm IP}_{\rm sd}$ corresponds to the contribution of multi-Pomeron interactions to diffraction production. This table demonstrates that most of the diffractive cross section in our model stems from the GW mechanism, this in accordance with the N = 4 SYM. A shortcoming of our approach is that we are unable to calculate distributions of the produced diffractive mass. This deficiency should be corrected, in view of the recent experimental activity at LHC, where missing mass distributions are planned to be measured in the near future [16]. The main goal of this paper is to suggest an approach which will allow us to calculate these mass distributions, based on new physical ideas.

Gribov partonic interpretation of the Pomeron [17] implies that the typical transverse momentum in the parton cascade that describes the Pomeron can be specified in a simple parton model by $q^2_\perp \approx 1/\alpha'_{\rm IP}$. Consequently, we believe that $\alpha'_{\rm IP} \simeq 0$ reflects the fact that the soft Pomeron is, actually, rather hard. The Donnachie-Landshoff Pomeron [18] has $\alpha'_{\rm IP} = 0.25\ {\rm GeV}^{-2}$ leading to a scale of hardness of approximately 4 GeV^2.

Our key idea is to view a soft interacting Pomeron as a hard probe that measures the quark and gluon contents of the hadron target, in our case a proton (see Fig. 1). We develop this idea, so as to be able to predict the mass distribution in diffraction production, with an additional assumption that the diffractive GW sector is initiated by Pomeron interactions with quarks within the hadron, while non-GW diffraction stems from Pomeron interactions with the hadronic target gluons.

Note that for $\Delta_{\rm IP} \simeq 0.3$ both mechanisms for diffraction production, i.e., GW and non-GW, lead to the production of diffractive mass whose values do not depend on the total energy [19]. Our suggested approach to the diffractive mass distribution recovers the widely used classification, in which the GW mechanism is responsible for diffraction in the region of relatively low mass, while non-GW mainly describes the production of high diffractive masses.

In the next section we present simple formulas that transcribe the above ideas to the diffractive mass distributions. We aim to predict these mass distributions in the LHC kinematic region. In Sec. III, we determine the scale of hardness for the Pomeron ($\tilde{Q}$), by comparing with the Tevatron data. We find the best value to be equal $\tilde{Q}^2 = 2\ {\rm GeV}^2$. In the conclusions we summarize our main results.

TABLE I. Predictions of our model for single diffractive production cross sections at different energies W.

$W = \sqrt{s}$ TeV	$\sigma^{\rm GW}_{\rm sd}$ (mb)	$\sigma^{\rm IP}_{\rm sd}$ (mb)	$\sigma_{\rm sd} = \sigma^{\rm GW}_{\rm sd} + \sigma^{\rm IP}_{\rm sd}$ (mb)
0.9	8.44	0.06	8.5
2.76	9.68	1.65	11.33
7	10.7	4.18	14.88
8	10.9	4.3	15.2
13	11.4	5.6	17

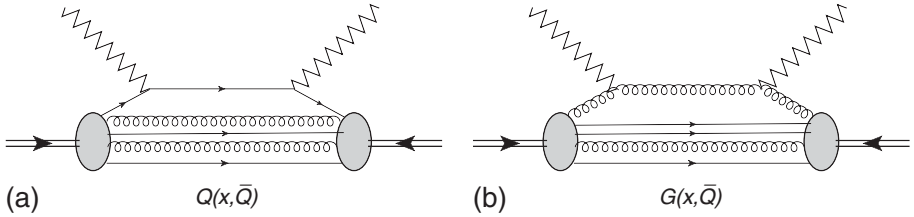

FIG. 1. The soft Pomeron as a hard probe Fig. 1(a) shows the interaction with quarks while the interaction with gluon is depicted in Fig. 1(b). The zigzag line denotes the Pomeron. The solid and helix lines show the quarks and gluons.

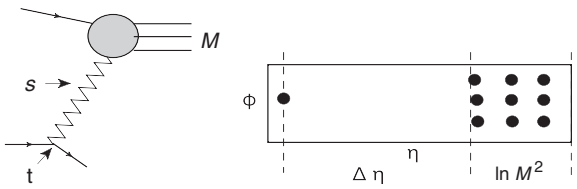

FIG. 2. Single diffractive production and related kinematic variables.

II. POMERON AS A HARD PROBE OF THE HADRON CONTENT

We assume that the soft Pomeron can be viewed as a hard probe with a scale of hardness $\bar{Q}$. This means that the Pomeron interacts with quarks and gluons as a composite [see Figs. 1(a) and 1(b)], in a way similar to that in which a virtual photon interacts in deep-inelastic scattering processes. Using this analogy we can write

$$\frac{d\sigma_{\rm sd}}{d\ln(M^2/M_0^2)} = \sigma_{\rm sd}^{\rm GW} q\left(\frac{\bar{Q}^2}{M^2+\bar{Q}^2},\bar{Q}^2\right)\Big/ I_q(M_{\rm max}) + \sigma_{\rm sd}^{\rm IP} g\left(\frac{\bar{Q}^2}{M^2+\bar{Q}^2},\bar{Q}^2\right)\Big/ I_g(M_{\rm max}). \tag{2.1}$$

In Eq. (2.1) $q(x)$ and $g(x)$ are the quark and the gluon distribution at the scale of hardness $\bar{Q}^2$. I_q and I_g are defined as

$$I_q = \int_{M_{\rm min}^2}^{M_{\rm max}^2} \frac{dM^2}{M^2} q\left(\frac{\bar{Q}^2}{M^2+\bar{Q}^2},\bar{Q}^2\right) \quad \text{and} \quad I_g = \int_{M_{\rm min}^2}^{M_{\rm max}^2} \frac{dM^2}{M^2} g\left(\frac{\bar{Q}^2}{M^2+\bar{Q}^2},\bar{Q}^2\right). \tag{2.2}$$

$M_{\rm max}$ and $M_{\rm min}$ are the maximal (minimal) mass that have been reached experimentally.

The energy variable (Bjorken x) for Pomeron-hadron scattering is equal to

$$0 = (p_{\rm IP}+p_p)^2 = -\bar{Q}^2 + x 2 p_{\rm IP}\cdot p_h, \qquad p_{\rm IP}^2 = -\bar{Q}^2,$$
$$(p_{\rm IP}+p_h)^2 = -\bar{Q}^2 + 2 p_{\rm IP}\cdot p_h, \qquad x = \frac{\bar{Q}^2}{M^2+\bar{Q}^2}. \tag{2.3}$$

$p_{\rm IP}$, p_h and p_p are the momenta of the Pomeron, the hadron and the parton (quark or gluon) with which the Pomeron interacts (see Fig. 1).

The value of $M_{\rm min}$ can be as small as $M_{\rm min} = m_h + m_\pi$. The value of $M_{\rm max}$ is bounded by the condition that we have a Pomeron exchange. As such, the value of $\Delta\eta$ that corresponds to the Pomeron exchange (see Fig. 2) should be large enough so that one can neglect the possible exchanges of the secondary Reggeons. In our initial analysis we took $\Delta\eta \geq 2$. Our model [1], with $\Delta\eta_{\rm min} = 2$, suggests that the contribution of the secondary Reggeons is approximately 50%. Note that the variable ξ which is usually introduced to describe diffraction production is equal to $\xi = 1 - x_L = M^2/s = \exp(-\Delta\eta)$. The choice of $\Delta\eta > 2$ implies that $\xi < 0.05$. At the LHC energies we took $M_{\rm min} = 1.1$ GeV and $M_{\rm max} = 200$ GeV, which corresponds to $\Delta\eta_{\rm min} = 7$. For this rapidity the contribution of the secondary Reggeons amounts to less than 10%.

In Figs. 3–5 we plot the predictions[1] for $M_{\rm max} = 200$ GeV and $M_{\rm min} = 1.1$ GeV. For $\bar{Q}^2$ we choose the value of 2 GeV^2 from the description of the CDF data [20] at the Tevatron (see the next section).

We wish to emphasize that the relative contribution of the quarks and gluons depends entirely on our model for soft interactions. However, the prediction turns out to be sensitive to both the value of the Pomeron's scale of hardness, and to the uncertainties in the gluon densities.

The resulting mass distribution depends on the Pomeron scale of hardness (see Fig. 6), where we plotted the prediction for $\bar{Q}^2 = 4$ GeV^2 and $\bar{Q}^2 = 2$ GeV^2. Note that, the quark contribution is less sensitive to the value of the Pomeron scale of hardness than to the gluon contribution, which depends crucially on $\bar{Q}$. There are large uncertainties in the gluon structure functions, since these have been extracted from the experimental data which are only indirectly connected to the gluon densities (see Fig. 7). It is possible that by measuring

[1]That numerical tables of our predicted mass distributions at LHC energies are obtainable from E. Levin.

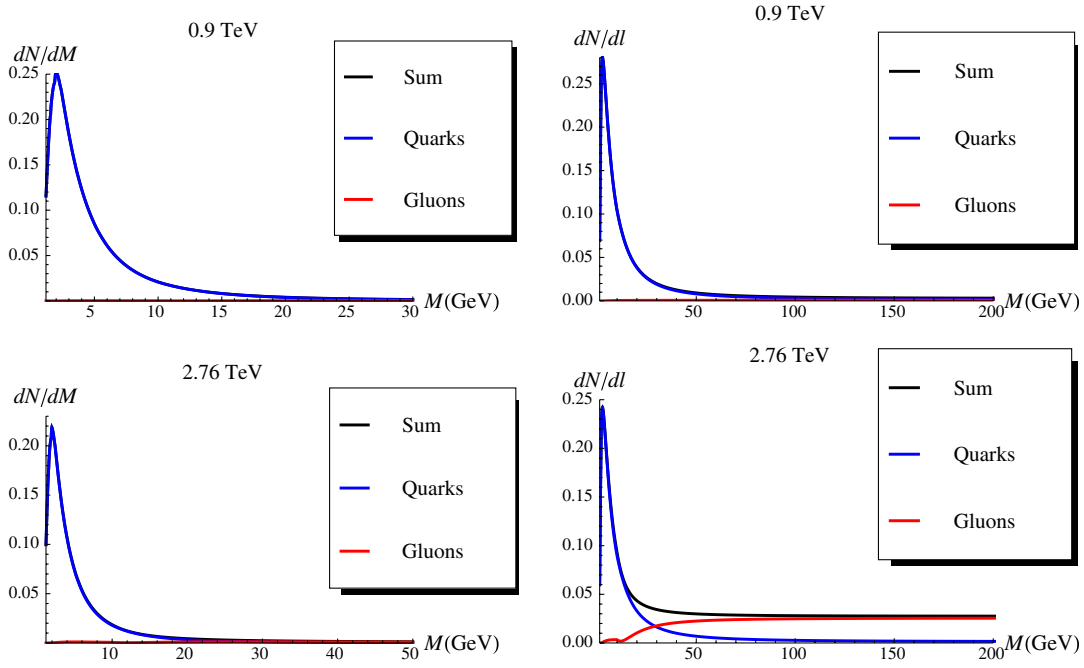

FIG. 3 (color online). dN/dM and dN/dl with $l = \ln(M^2/M^2_{\rm min})$ versus M for energies $W = 0.9$ and 2.76 TeV. For the quark and gluon structure functions from the H1-Zeus combined fit (HERAPDF01) [22] is used. The scale of hardness for the Pomeron is taken $\tilde{Q} = 1.42$ GeV.

$dN/d\ln(M^2/M_0^2)$, one will obtain useful information on the leading order gluon densities. On the other hand, the low mass distributions that depend on the quark densities do not suffer from such uncertainties, and can be predicted rather accurately (see Fig. 8).

III. COMPARISON WITH THE EXPERIMENTAL DATA

The mass distribution for single diffractive production has only been measured at low energies; however, we

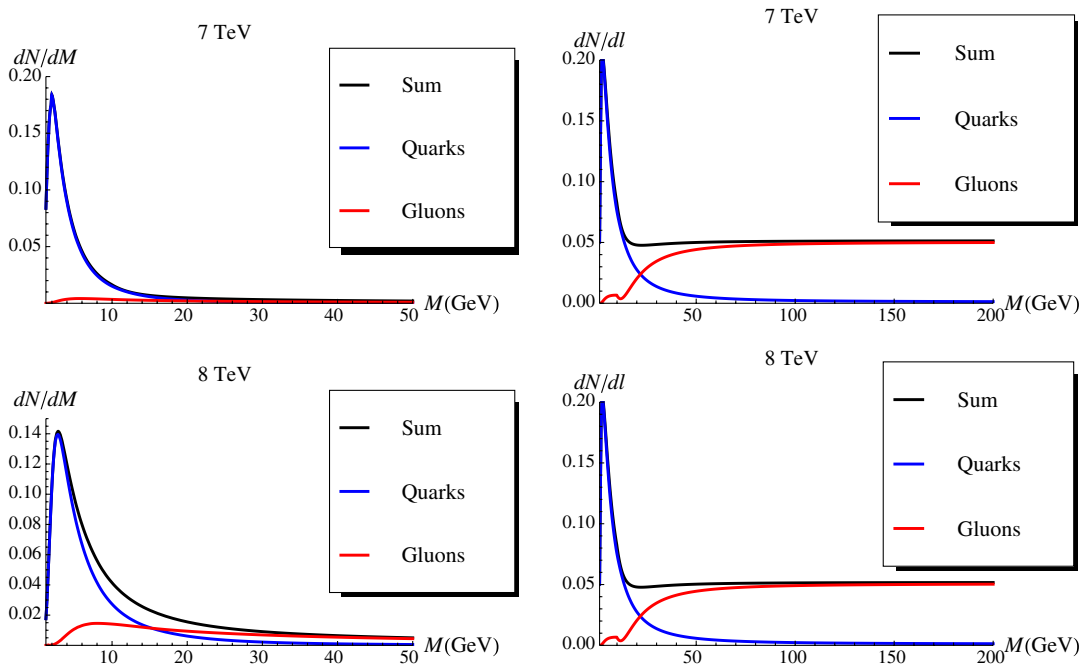

FIG. 4 (color online). dN/dM and dN/dl with $l = \ln(M^2/M^2_{\rm min})$ versus M for energies $W = 7$ and 8 TeV. For the quark and gluon structure functions from the H1-Zeus combined fit (HERAPDF01) [22] is used. The scale of hardness for the Pomeron is taken $\tilde{Q} = 1.42$ GeV.

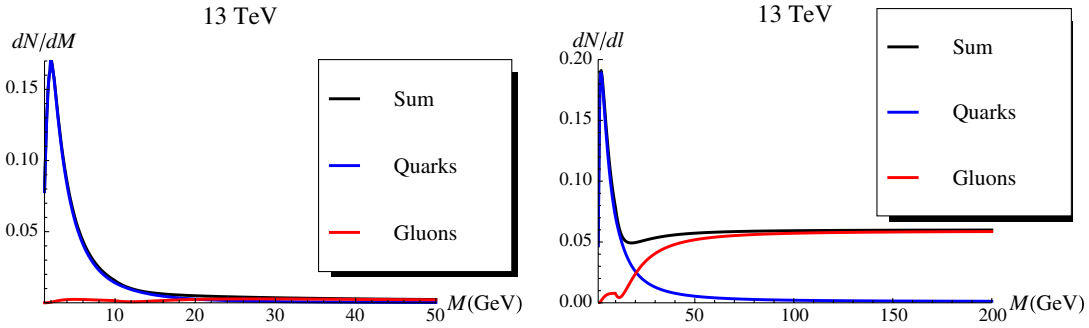

FIG. 5 (color online). dN/dM and dN/dl with $l = \ln(M^2/M_{\min}^2)$ versus M at $W = 13$ TeV. For quark and gluon structure functions the H1-Zeus combined fit (HERAPDF01) [22] is used. The scale of hardness for the Pomeron is taken $\bar{Q} = 1.42$ GeV.

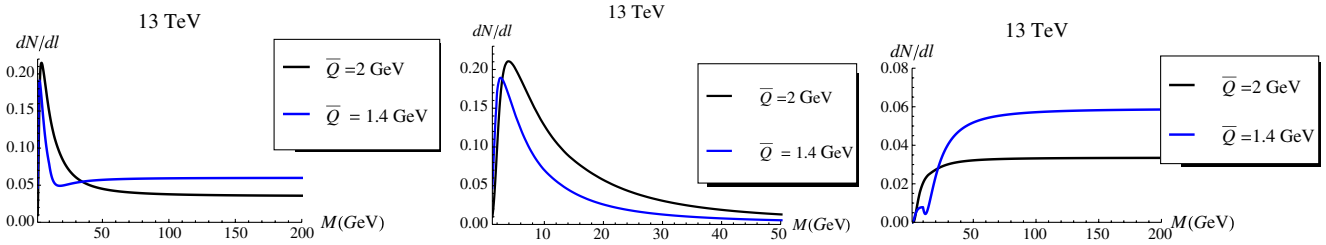

FIG. 6 (color online). dN/dl with $l = \ln(M^2/M_{\min}^2)$ versus M at $W = 13$ TeV for different scales of hardness for Pomeron ($\bar{Q}$).

compare with the data obtained at the Tevatron [20,21], and found even this data base is not adequate to determine the Pomeron contribution. Even though one can produce at the Tevatron large diffractive masses, up to $M = 360$ GeV, we find that the contribution of the secondary Reggeons is significant, about 50% given $\Delta\eta_{\min} = 2$. We conclude that taking $\Delta\eta_{\min} = 2$ is not sufficient to induce a strong enough suppression of the secondary Reggeons contribution to single diffraction. We note that, diffractive $M = 400$ GeV produced at the LHC corresponds to $\Delta\eta = 6$. Therefore, we will have to wait for the diffractive mass distribution at the LHC to discuss the Pomeron induced diffractive production. In Fig. 9 we plot the CDF data and our estimates. One can see from this comparison that the data support a scale of hardness for the Pomeron $\bar{Q}^2 = 2$ GeV^2. Bearing in mind all uncertainties that stem from the gluon structure function and the contribution of the secondary Reggeons, which could change the behavior at large ξ, we consider that our attempt to describe the data is rather successful.

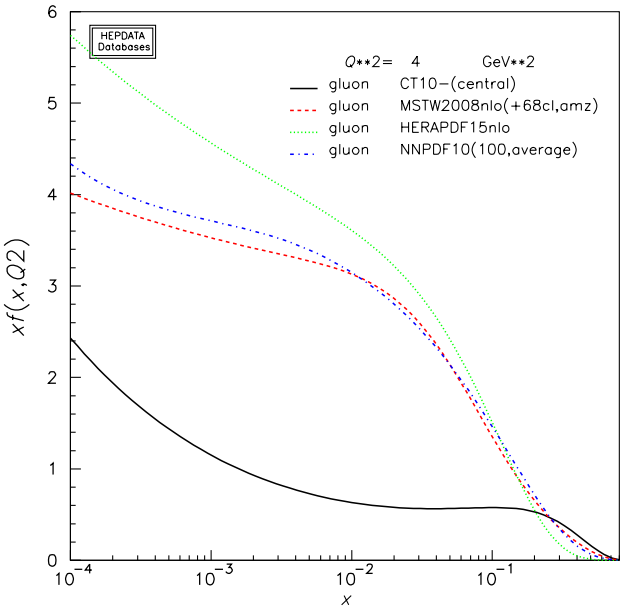

FIG. 7 (color online). Gluon densities for different parametrizations. The figure is taken from Durham HEP data [23].

It is important to mention that for this comparison we require more input from our model. To this end, we use the value of the single diffraction slope $B_{\rm sd}^{\rm GW} = 6.36$ GeV^{-2} (see Ref. [1]. This slope has been calculated for the single diffractive GW sector. For the non-GW diffractive Pomeron sector, the slope is the same as $B_{\rm sd}^{\rm GW}$. For the description of the CDF data we use the following formula:

$$\frac{d\sigma_{\rm sd}}{d\xi dt} = \frac{s}{M^2}\left\{B_{\rm sd}^{\rm GW}\exp(B_{\rm sd}^{\rm GW}t)\sigma_{\rm sd}^{\rm GW}q\left(\frac{\bar{Q}^2}{M^2+\bar{Q}^2},\bar{Q}^2\right)\Big/ I_q(M_{\max}) + (B_{\rm sd}^{\rm IP}\exp(B_{\rm sd}^{\rm IP}t)\sigma_{\rm sd}^{\rm IP}g\left(\frac{\bar{Q}^2}{M^2+\bar{Q}^2},\bar{Q}^2\right)\Big/ I_g(M_{\max})\right\}. \quad (3.1)$$

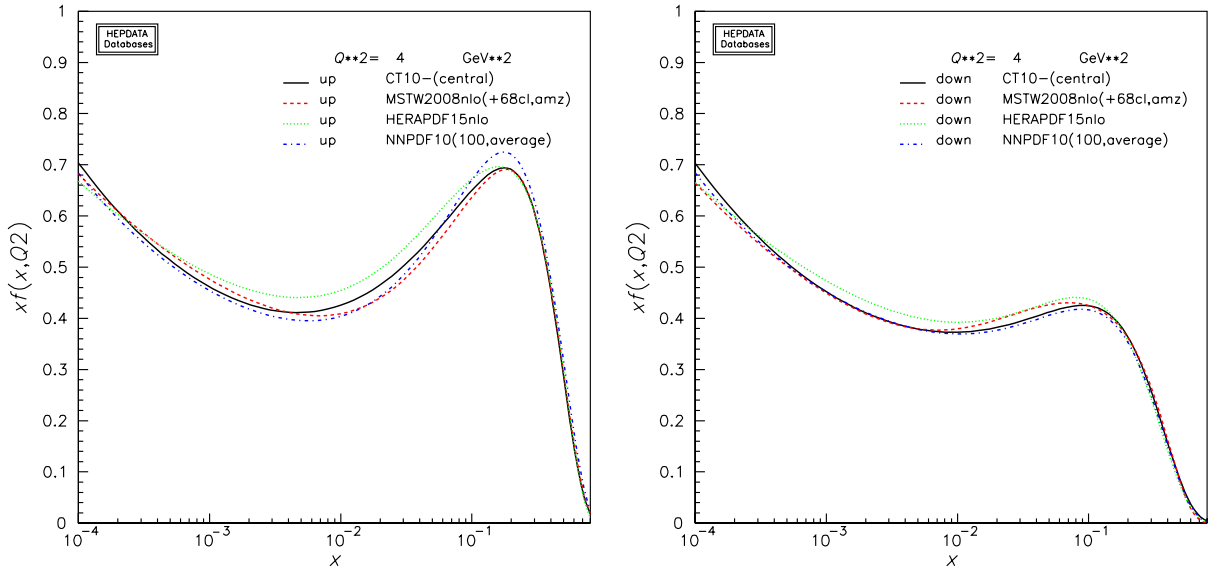

FIG. 8 (color online). Quark densities for different parametrizations. The figure is taken from Durham HEP data [23].

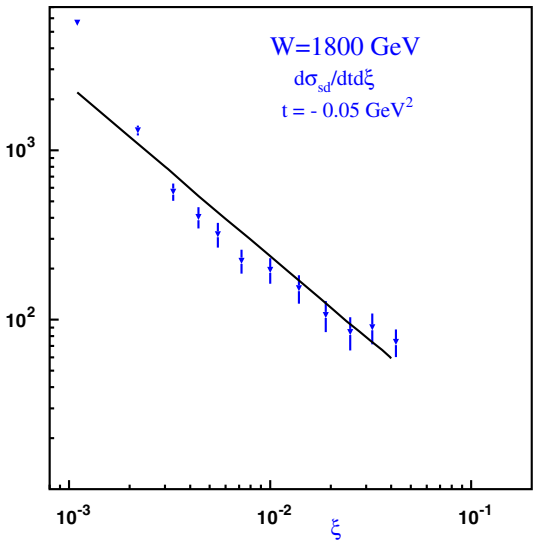

FIG. 9 (color online). The comparison with the CDF data [20,21] at the Tevatron. $\xi = M^2/s$. The scale of hardness for the Pomeron is taken to be equal to $\tilde{Q}^2 = 2$ GeV^2.

IV. CONCLUSIONS

This paper was triggered by the absence of a theoretical procedure to calculate the single diffractive mass distribution. Such a procedure is an essential ingredient in the forthcoming experimental analysis of the mass distribution in the diffractive channels, foremost the leading single diffraction channel. To rectify this deficiency, we have suggested that the Pomeron that has been adopted in Refs. [1–3], stems from processes with sufficiently large transverse momenta, and can be viewed as a hard probe of the constituents of the hadron. The simple formula of Eq. (2.1) indicates how we can use the mass distribution of single diffraction production, to measure the quarks and gluons in a hadron. We trust that these will be helpful in understanding the soon to be available experimental diffractive mass data from the LHC.

We believe that the description of $dN_{\rm sd}/d\ln(M^2/M_0^2)$ in terms of quarks and gluons will determine the Pomeron scale of hardness, as well as additional information on the gluon densities.

ACKNOWLEDGMENTS

We thank Risto Orava, Martin Poghosyan, and Jean-Pierre Charles Revol for discussions on the experimental situation in diffractive production. This research was supported by the Fondecyt (Chile) Grant No. 1100648.

[1] E. Gotsman, E. Levin, and U. Maor, Phys. Lett. B **716**, 425 (2012); Phys. Rev. D **85**, 094007 (2012).

[2] E. Gotsman, E. Levin, and U. Maor, Eur. Phys. J. C **71**, 1553 (2011).

[3] E. Gotsman, E. Levin, U. Maor, and J. S. Miller, Eur. Phys. J. C **57**, 689 (2008).

[4] E. Gotsman, E. Levin, and U. Maor, Phys. Rev. D **84**, 051502 (2011); **81**, 051501 (2010).

[5] F. E. Low, Phys. Rev. D **12**, 163 (1975); S. Nussinov, Phys. Rev. Lett. **34**, 1286 (1975); E. A. Kuraev, L. N. Lipatov, and V. S. Fadin, Sov. Phys. JETP **45**, 199 (1977); I. I. Balitsky and L. N. Lipatov, Sov. J. Nucl. Phys. **28**, 822 (1978); A. H. Mueller, Nucl. Phys. **B415**, 373 (1994); **B437**, 107 (1995); L. V. Gribov, E. M. Levin, and M. G. Ryskin, Phys. Rep. **100**, 1 (1983); A. H. Mueller and J. Qiu, Nucl. Phys. **B268**, 427 (1986); L. McLerran and R. Venugopalan, Phys. Rev. D **49**, 2233 (1994); **49**, 3352 (1994); **50**, 2225 (1994); **53**, 458 (1996); **59**, 094007 (1999); L. N. Lipatov, Phys. Rep. **286**, 131 (1997); Sov. Phys. JETP **63**, 904 (1986), and references therein.

[6] I. Balitsky, Nucl. Phys. **B463**, 99 (1996); Y. Kovchegov, Phys. Rev. D **60**, 034008 (1999).

[7] J. Jalilian-Marian, A. Kovner, A. Leonidov, and H. Weigert, Phys. Rev. D **59**, 014014 (1998); Nucl. Phys. **B504**, 415 (1997); E. Iancu, A. Leonidov, and L. D. McLerran, Phys. Lett. B **510**, 133 (2001); Nucl. Phys. **A692**, 583 (2001); H. Weigert, Nucl. Phys. **A703**, 823 (2002).

[8] Y. Kovchegov and E. Levin, *Quantum Choromodynamics at High Energies* (Cambridge University Press, Cambridge, 2012), and references therein.

[9] A. V. Kotikov, L. N. Lipatov, A. I. Onishchenko, and V. N. Velizhanin, Phys. Lett. B **595**, 521 (2004); **632**, 754 (2006), and references therein.

[10] R. C. Brower, J. Polchinski, M. J. Strassler, and C. I. Tan, J. High Energy Phys. 12 (2007) 005; R. C. Brower, M. J. Strassler, and C. I. Tan, J. High Energy Phys. 03 (2009) 050.

[11] Y. Hatta, E. Iancu, and A. H. Mueller, J. High Energy Phys. 01 (2008) 026.

[12] L. Cornalba and M. S. Costa, Phys. Rev. D **78**, 096010 (2008); L. Cornalba, M. S. Costa, and J. Penedones, J. High Energy Phys. 06 (2008) 048; 09 (2007) 037.

[13] B. Pire, C. Roiesnel, L. Szymanowski, and S. Wallon, Phys. Lett. B **670**, 84 (2008).

[14] E. Levin, J. Miller, B. Z. Kopeliovich, and I. Schmidt, J. High Energy Phys. 02 (2009) 048.

[15] M. L. Good and W. D. Walker, Phys. Rev. **120**, 1857 (1960).

[16] Jean-Pierre Charles Revol of the ALICE Collaboration and Risto Orava of the TOTEM Collaboration (private communication).

[17] V. N. Gribov, arXiv:hep-ph/0006158; Yad. Fiz. **9**, 640 (1969) [Sov. J. Nucl. Phys. **9**, 369 (1969)].

[18] A. Donnachie and P. V. Landshoff, Nucl. Phys. **B231**, 189 (1984); Phys. Lett. B **296**, 227 (1992); Z. Phys. C **61**, 139 (1994).

[19] G. Gustafson, Phys. Lett. B **718**, 1054 (2013).

[20] F. Abe *et al.* (CDF Collaboration), Phys. Rev. D **50**, 5535 (1994).

[21] K. A. Goulianos and J. Montanha, Phys. Rev. D **59**, 114017 (1999).

[22] F. D. Aaron *et al.* (H1 and ZEUS Collaborations), J. High Energy Phys. 01 (2010) 109.

[23] Durham HepData repository, http://hepdata.cedar.ac.uk/pdfs.